

Comparing Design Ground Snow Load Prediction in Utah and Idaho

Brennan Bean¹, Marc Maguire A.M.ASCE², and Yan Sun³

ABSTRACT

Snow loads in the western United States are largely undefined due to complex geography and climates, leaving the individual states to publish detailed studies for their region, usually through the local Structural Engineers Association (SEAs). These associations are typically made up of engineers not formally trained to develop or evaluate spatial statistical methods for their regions and there is little guidance from ASCE 7. Furthermore, little has been written to compare the independently developed design ground snow load prediction methods used by various western states. This paper addresses this topic by comparing the accuracy of a variety of spatial methods for predicting 50 year (i.e. design) ground snow loads in Utah and Idaho. These methods include, among others, the current Utah snow load equations, Idaho's normalized ground snow loads based on inverse distance weighting, two forms of Kriging, and the authors' adaptation of PRISM. The accuracy of each method is evaluated by measuring the mean absolute error using ten fold cross validation on datasets obtained from Idaho's 2015 snow load report, Utah's 1992 snow load report, and a new Utah ground snow load dataset. These results show that regression-based Kriging and PRISM methods have the lowest cross validated errors across all three datasets. These results also show that normalized ground snow loads, which are a common way of accounting for elevation in traditional interpolation methods, do not fully account for the effect of elevation on ground snow

¹PhD Student, Department of Mathematics and Statistics, Utah State University, 3900 Old Main Hill, Logan, UT 84322, Email: brennan.bean@aggiemail.usu.edu

²Assistant Professor, Department of Civil and Environmental Engineering, Utah State University, 4110 Old Main Hill, Logan, Utah 84321

³Assistant Professor, Department of Mathematics and Statistics, Utah State University, 3900 Old Main Hill, Logan, UT 84322

20 loads within the considered datasets. The methodologies and cautions outlined in this paper provide
21 a framework for an objective comparison of snow load estimation methods for a given region as
22 state SEAs look to improve their future design ground snow predictions. Such comparisons will
23 aid states looking to amend or improve their current ground snow load requirements.

24 INTRODUCTION

25 Heavy snowstorms in the winter of 2017 filled local newspapers across the western United
26 States with reports of snow related building collapses and fatalities (Lafferty 2017, Associated
27 Press 2017, Mieux 2017, Kato and Florio 2017, Fisicaro 2017, Glover 2017). These snow-related
28 failures can be catastrophic to local economies, like the recent \$100 million in losses incurred
29 by Idaho/Oregon's onion industry (Ellis 2017). One study of 40 snow-induced building failures
30 reported an average cost of \$166 per square meter and 122 days of business interruption for repairs
31 (Strobel and Liel 2013). Snow-related damages can extend beyond building repairs, as a study of
32 1,100 domestic and international snow-induced building failures reported more than 300 fatalities
33 (Geis et al. 2011). Few details are made public about the true causes of the above damages, as
34 they could be agricultural buildings not designed to code or even suffer from construction error,
35 but these reports and articles provide a sample of the serious consequences associated with snow
36 load prediction.

37 Subtler costs are also associated with overly conservative load designs. As articulated by Nowak
38 and Collins (2012): "Conceptually, we can design [a] structure to reduce the probability of failure,
39 but increasing the safety... beyond a certain optimum level is not always economical." The following
40 two examples demonstrate this point by exploring the relationship between design snow loads and
41 roof construction costs. Roof costs are selected for these illustrations as they are likely the aspect
42 of a structure most sensitive to snow load design.

43 The first example is found in the 2017 Craftsman National Building Cost Manual, which
44 includes a table of estimated roof costs for manufactured homes rated for different snow loads.
45 In this manual, a doubling of the roof snow load requirement from 1.44 to 2.88 kPa results in an
46 approximate threefold increase in the estimated cost per unit meter of roof (\$11 to \$36) (Moselle

47 2016). While increases in cost outside the selected load range are not quite as drastic, the example
48 demonstrates the influence of snow loads on roof costs. The second example comes from roof
49 joist costs provided to the authors by Vulcraft Utah (Brigham City, Utah) in January 2018. These
50 roof-only designs assume varying snow loads with the constant depths, typical joist spacings and
51 a L/240 deflection limit, as indicated in Figure 1. These costs do not include the effects of the
52 snow and larger roof components on the remainder of the gravity or seismic systems' cost. For this
53 system, doubling the roof snow load requirement from 1.44 to 2.88 kPa leads to a 40-90% increase
54 in the cost of the joists.

55 These two examples may represent highly sensitive situations with respect to cost and snow
56 load. Other systems and components would likely not experience such dramatic cost increases. Re-
57 gardless, the potential economic burdens created by overly conservative requirements likely explain
58 recently amended ground snow load requirements in Rich County, Utah, where new requirements
59 for major communities in the county (approximately 2.73 kPa) are less than half of those dictated
60 previously (6.3-7.2 kPa) (Utah 2016).

61 American Society of Civil Engineers (ASCE) design ground snow load requirements have
62 historically remained largely unspecified for the topographically complex western states up through
63 ASCE 7-10 (ASCE 2013). This had led to the creation of a diverse set of state specific snow
64 load estimation methods (Sack 2015). New snow load tables provided for many of the western
65 states in ASCE 7-16 are derived from these state snow load reports (ASCE 2017). Design ground
66 snow loads are defined in this paper as estimated 50 year ground snow loads. With the exception
67 of the reliability-based snow loads in Colorado (Torrents et al. 2016), this definition is consistent
68 with ASCE-7 and western state snow load reports. Many of these reports (or portions of them)
69 are freely available to the public (NACSE 2012, SEAU 1992, Torrents et al. 2016, Al Hatailah
70 et al. 2015, Theisen et al. 2004) and provide a wealth of information on dataset development,
71 model predictions, and implications for building design. However, little is written regarding the
72 accuracy of the methods used to predict design ground snow loads. While Sack (2015) and Sack
73 et al. (2016) discuss differences between state methodologies and acknowledge discrepancies in

74 predictions along state boundaries, no formal comparison of design ground snow load prediction
75 methods is found in the literature. A lack of accuracy comparisons makes it difficult to determine
76 whether differences in design ground snow load requirements along state boundaries are caused by
77 differences in methodology, data, or both.

78 This paper begins such comparisons by determining the cross validated accuracies of several
79 design ground snow load prediction methods on three independently developed datasets. These
80 cross validation results are calculated using the R statistical software environment (R Core Team
81 2017) and visualized with the ggplot2 (Wickham 2009) and RColorBrewer (Neuwirth 2014) pack-
82 age extensions. These results will be preceded by a summary of the datasets and spatial prediction
83 methods used in the comparisons and followed by a discussion of the challenges and limitations in
84 predicting design ground snow loads. The authors conclude that regression-based spatial estimators
85 that model the log-linear relationship between ground snow load and elevation consistently out-
86 perform all other methods in terms of minimizing the cross validated mean absolute error (MAE).
87 Cross validation also highlights some of the limitations of normalized ground snow loads (NGSL),
88 as explained in the "Prediction Comparisons" section of this paper. These results in Utah and
89 Idaho provide a framework for a formal comparison of methodologies used by each of the western
90 states, an important step for states looking to amend or improve their current ground snow load
91 requirements.

92 DATA

93 The three datasets used in the cross validation comparisons are the authors' new Utah dataset
94 (UT-2017), the 1992 Utah snow load report dataset (UT-1992) and the 2015 Idaho snow load report
95 dataset (ID-2015). The variable of interest in each dataset is the design ground snow load. These
96 design ground snow loads are calculated by fitting the annual maximum snow water equivalents
97 (SWE) at each station location to a probability distribution and extracting the 98th percentile.
98 Nearly all low elevation stations do not provide direct measurements of SWE. At locations where
99 SWE is not measured, estimates of SWE are made from snow depth measurements using either
100 the Rocky Mountain Conversion Density (RMCD) (Sack and Sheikh-Taheri 1986), or an equation

101 developed by Sturm et al. (2010) referred to hereafter as "Sturm's equation". Table 1 provides an
102 overview of the methods used to estimate design ground snow loads within each dataset. These
103 readily available datasets were selected to compare the effectiveness of various spatial methods
104 in predicting ground snow loads for different climates, terrain, and station coverage. In addition,
105 the development of each of considered spatial method is associated with one of these datasets,
106 including the current Utah snow load equations (UT-1992), Idaho's normalized ground snow loads
107 based on inverse distance weighting (ID-2015), Kriging (UT-2017) and PRISM (UT-2017). The
108 consideration of these three independently developed data sources ensures that the cross validation
109 comparisons are not limited to one isolated dataset.

110 Each of these datasets use observations from Natural Resources Conservation Service (NRCS)
111 Snowpack Telemetry (SNOTEL) and Snow Course (SC) stations, as well as data from the National
112 Weather Service (NWS) cooperative observer network (COOP). Many SNOTEL stations were in-
113 stalled to replace discontinued SC stations, thus creating situations where two separate stations have
114 the same location. Identical decimal degree locations for two distinct stations creates singularity
115 issues in many spatial interpolation methods. This problem was resolved by adding an arbitrarily
116 small number r , ($|r| < .001$) to the decimal degree locations to create well defined but negligible
117 spatial separation between such stations.

118 Figure 2 (a-c) reveals the distinct log-linear relationship between station design ground snow
119 load estimates and elevation for each dataset. These scatterplots include lines representing ordinary
120 and generalized least squares regression estimates of this log-linear relationship (using elevation as
121 the predictor). The development of these regression lines will be discussed further in the "Methods"
122 section of this paper. In addition, the histogram of station elevations in Figure 2 (d) show that the
123 Idaho dataset contains a larger proportion of high elevation stations than either Utah dataset. Cross
124 validated results must be interpreted in the context of station elevation, as higher elevations tend to
125 have higher snow loads and consequently more variability in predictive accuracy.

The New Utah Dataset (UT-2017)

This dataset contains 279 (192 COOP, 87 SNOTEL) Utah stations with an additional 136 stations (103 COOP, 33 SNOTEL), all located within 100km of the Utah border. Log-normal distribution parameter estimates were calculated using annual yearly maximums for years 1970 to 2017 via maximum likelihood estimation. This range focuses on years where SNOTEL station measurements are available, as the earliest available measurements from active SNOTEL stations in Utah is 1978 (NRCS 2017). Sturm's equation estimated SWE from snow depth when SWE measurements were missing. This equation is defined using the coefficients for a "prairie" and "alpine" terrains (Sturm et al. 1995) as

$$SWE_i = \begin{cases} h_i [.3608 * (1 - \exp(-.0016h_i - .0031d_i)) + .2332] & \text{Elevation} < 2113.6\text{m} \\ h_i [.3738 * (1 - \exp(-.0012h_i - .0038d_i)) + .2237] & \text{Elevation} \geq 2113.6\text{m} \end{cases} \quad (1)$$

where h_i represents snow depth (in centimeters) and d_i represents the day of the snow year, ranging from -92 (October 1) to 181 (June 30), for any given observation i (2010). See Bean et al. (2018) for a copy of this dataset along with further details regarding its creation.

The 1992 Utah Dataset (UT-1992)

These data consist of 413 stations (210 SC, 203 COOP), all located in Utah. The method used to calculate the Log-Pearson type III parameters is not specified. Estimates of SWE using the RMCD were occasionally adjusted when the resulting snow water equivalents exceeded the station's winter cumulative precipitation. Tables of these data can be found in the Utah snow load report (SEAU 1992).

The 1992 Utah report does not provide precise station locations. Since 1979, many of the snow course stations used in this report have been discontinued, and precise location information is unavailable. Station locations were determined for all but seven stations through a combination of station number matching in NRCS and NWS station databases, as well as personal contact with Randall Julander at the Utah Snow Survey Office in Salt Lake City. Locations for the

150 seven remaining stations were approximated using Google Earth to determine coordinates given
151 approximate station location information from the snow survey office and county information given
152 in the 1992 Utah report.

153 **The 2015 Idaho Dataset (ID-2015)**

154 These data consist of 394 (246 SC/SNOTEL, 148 COOP) Idaho stations with an additional 257
155 (222 SC/SNOTEL, 35 COOP) located near the Idaho border with the most recent measurements
156 being taken in 2014. Log-Pearson type III distribution parameter estimates were determined using
157 the sample mean, standard deviation skew of annual of yearly maximums at each station location
158 (i.e. method of moments). The data and further details regarding the estimation of these 50 year
159 events are given in Al Hataillah's Masters Thesis (2015).

160 **METHODS**

161 Each of the following methods predict design ground snow loads at a state level using design
162 ground snow loads at surrounding station locations as input. These methods were selected due
163 to their ability to be easily applied to datasets of varying size and location, an important pre-
164 requisite for calculating the cross validated errors discussed later in this paper. Details of the
165 following methods can be found at citations provided in the respective summaries. For comparative
166 convenience, the primary methods of consideration are defined using a common set of notation.
167 Let $p_g(\mathbf{u})$ denote the ground snow load at a location \mathbf{u} (with p_g^* representing the predicted design
168 ground snow load) and let $A(\mathbf{u})$ denote location elevation. Further, let \mathbf{u}_α represent the location of
169 station α ($\alpha = 1, \dots, N$) and let $D(\mathbf{u}_i, \mathbf{u}_j)$ represent the geographic distance between locations \mathbf{u}_i
170 and \mathbf{u}_j .

171 The defining feature of each method is in the way that elevation is accounted for in the design
172 ground snow load predictions. With the exception of the ground snow load equations in the 1992
173 Utah Snow load report, each of the considered methods use normalized ground snow loads (NGSL)
174 or some variant of linear regression. Normalized ground snow loads (NGSL) are calculated as
175 design ground snow load divided by elevation $\left(\frac{p_g^*(\mathbf{u}_\alpha)}{A(\mathbf{u}_\alpha)}\right)$. They "appear to mask out the effects of
176 the environment on the snow-making mechanism" and "reduce the entire area to a common base

177 elevation" (Sack et al. 2016). NGSL have a long history of use in western state snow load studies,
178 including the current snow load reports of Idaho, Montana and Washington (Sack et al. 2016).

179 On the other hand, regression based estimators seek to characterize the log-linear relationship
180 between design ground snow loads and elevation observed in Figure 2. This relationship can be
181 characterized using simple linear regression (LR) defined as

$$182 \log(p_g^*(\mathbf{u})) = \beta_0 + \beta_1 A(\mathbf{u}) \quad (2)$$

183 where β_0 and β_1 are calculated using ordinary least squares regression. The cross validated results
184 in the following section show that differences in method accuracy can be largely attributed to
185 differences in the characterization of the elevation/snow load relationship.

186 **Current Utah Ground Snow Load Equations**

187 The Structural Engineers Association of Utah (SEAU) predict design ground snow loads from
188 elevation using the following equation (referred to hereafter as SNLW):

$$189 p_g^*(\mathbf{u}) = \begin{cases} \left(P_0^2 + S^2 (A(\mathbf{u}) - A_0)^2 \right)^{\frac{1}{2}} & A(\mathbf{u}) > A_0 \\ P_0 & A(\mathbf{u}) \leq A_0 \end{cases} \quad (3)$$

190 where P_0 (base ground snow load), S (change in ground snow load with elevation), and A_0 (base
191 ground snow elevation) are parameters whose values are uniquely defined for each county. County
192 specific parameters were selected to be "an approximate upper bound" to both the design ground
193 snow loads and the maximum observed ground snow loads for the set of stations in and near the
194 county of interest (SEAU 1992).

195 Recently amended snow load requirements for the state replace the equation estimates at select
196 locations in Utah (Utah 2016). These updated requirements generally result in a reduction of
197 ground snow loads when compared to the original equation estimates (Bean et al. 2017).

Inverse Distance Weighting

In Idaho's normalized ground snow loads based on inverse distance weighting (IDW), the predicted ground snow load at a particular location is a weighted average of the NGSL of surrounding stations, multiplied by the location's elevation. This prediction is expressed as

$$p_g^*(\mathbf{u}) = \frac{A(\mathbf{u})}{\sum_{\alpha=1}^N D(\mathbf{u}_\alpha, \mathbf{u})} \sum_{\alpha=1}^n \left[\left(\frac{1}{D(\mathbf{u}_\alpha, \mathbf{u})} \right)^c \frac{p_g^*(\mathbf{u}_\alpha)}{A(\mathbf{u}_\alpha)} \right]. \quad (4)$$

The variable c allows for adjustments to the weighting factor, with larger values of c further reducing the influence of stations far away from the area of interest. The Idaho snow load report uses $c_1 = 2$ for locations with elevations below 1,219 m (4,000 ft) and $c_2 = 6$ for locations with elevations above $l = 1,219\text{m}$ (Al Hatailah et al. 2015). The cross validation results for all three datasets in the following sections use these parameter values. One key difference in this implementation is the use of geographic distances rather than euclidean distances from the Idaho Transverse Mercator Projection (Al Hatailah 2015). The use of geographic distances eliminates the spatial distortion that may occur when applying a euclidean based map projection to a large geographical area.

Linear Triangulation Interpolation

In linear triangulation interpolation (TRI), the area of interest is partitioned into a set of non-intersecting triangles with vertices at each station location. Predictions use a weighted average of the NGSL at the three stations forming the triangle overlaying the point of interest (Akima 1978). The R implementation of this strategy creates an entire grid of predicted values within the convex hull of the given data points (Akima and Gebhardt 2015). There are instances during cross validation when the convex hull of the training set does not encompass points in the test set, resulting in missing value predictions. These missing values are currently ignored when computing cross validated errors. These missing value predictions would need to be addressed prior to any serious consideration of this method in future work.

221 **PRISM**

222 PRISM (Parameter-elevation Relationships on Independent Slopes Model) uses weighted least
223 squares regression to account for additional climatological factors in response variable predictions
224 (Daly et al. 2002, 2008). This leads to an extension of Equation 2 with the form

$$225 \log(p_g^*(\mathbf{u})) = \beta_0(\mathbf{u}, \mathbf{X}) + \beta_1(\mathbf{u}, \mathbf{X})A(\mathbf{u}) \quad (5)$$

226 where $\beta_0(\mathbf{u}, \mathbf{X})$ and $\beta_1(\mathbf{u}, \mathbf{X})$ are estimated via weighted least squares regression. Final predictions
227 exponentiate the log-scale predictions. The regression weights are a function of several factors
228 defined in this adaptation of the algorithm as

$$229 \mathbf{W}(\mathbf{u}, \mathbf{X}) = \mathbf{W}_c [F_d \mathbf{W}_d^2 + F_z \mathbf{W}_z^2]^{\frac{1}{2}} \mathbf{W}_b, \quad (6)$$

230 where \mathbf{X} is the matrix containing all station meta-data and

- 231 • \mathbf{W}_c - a cluster factor (stations distributed in a tight cluster and similar in elevation receive
232 less weight)
- 233 • \mathbf{W}_d - distance weighting (stations closer to the area of interest receive more weight)
- 234 • \mathbf{W}_z - elevation weighting (stations with altitudes similar to the area of interest receive more
235 weight)
- 236 • \mathbf{W}_b - basin weighting (stations located in the same water basin as the area of interest receive
237 more weight)
- 238 • F_d and F_z - importance factors for distance weighting and elevation respectively

239 These weights create a unique linear model fit for each area of interest. For details regarding the
240 calculation of these weights, refer to (Bean et al. 2017) with one noted difference. Originally the
241 basin weights compared similarities in station watersheds from the United States Geologic Survey
242 (USGS) Hydrologic Unit Codes (HUC) 2-12 (USGS 2016). These finest watershed levels (HUC
243 10 and 12) proved too small to be relevant in the weighting scheme, as nearly every station had

244 its own HUC 12 designation. This in mind, the basin weighting function now only detects more
 245 coarse water basin associations in the following manner:

$$246 \quad \mathbf{W}_{b_\alpha} = \left(\frac{s_\alpha + 1}{5} \right)^c, \quad (7)$$

247 where s represents the number of common watersheds (*four* levels ranging from HUC 2 through
 248 8) shared by station α and the target grid cell, and c is a user defined weighting factor that changes
 249 the shape of the weighting function.

250 **Kriging**

251 The family of Kriging estimators leverage the spatially dependent correlations between observa-
 252 tions to make predictions. The gstat package extension of R (Pebesma 2004) provides a numerical
 253 implementation of many Kriging variations. Details regarding these family of estimators are given
 254 in Goovaerts (1997), and motivate the notation used in this paper. One Kriging extension of
 255 Equation 2 is called Simple Kriging with varying Local Means (SKLM) (Goovaerts 2000) defined
 256 symbolically as

$$257 \quad \log(p_g^*(\mathbf{u})) = \beta_0 + \beta_1 A(\mathbf{u}) + \sum_{\alpha=1}^N \lambda_\alpha(\mathbf{u}) r(\mathbf{u}_\alpha). \quad (8)$$

258 This method proceeds in three steps. First, a linear model is calculated identical to Equation 2.
 259 Then, simple kriging uses the residuals of the linear model to predict a residual value at the location
 260 of interest. Finally, this residual value is used to update the original linear model prediction. The
 261 simple kriging coefficients ($\lambda_\alpha(\mathbf{u})$) are calculated by solving the kriging system

$$262 \quad \sum_{\alpha=1}^N \lambda_\beta(\mathbf{u}) C_R(D(\mathbf{u}_\alpha, \mathbf{u}_\beta)) = C_R(D(\mathbf{u}_\alpha, \mathbf{u})) \quad \beta = 1, \dots, n. \quad (9)$$

263 where C_R represents the covariance between any two observations and is assumed to be a function
 264 of distance.

265 An alternative method for accounting for elevation in kriging predictions is through universal
 266 kriging (UK), which calculates the trend implicitly within the kriging system, rather than separately

267 as in SKLM (Goovaerts 1997). When elevation is the only trend coefficient, the universal kriging
 268 estimates are equivalent to

$$269 \quad \log(p_g^*(\mathbf{u})) = \beta_0^* + \beta_1^* A(\mathbf{u}) + \sum_{\alpha=1}^N \lambda_{\alpha}(\mathbf{u}) r(\mathbf{u}_{\alpha}) \quad (10)$$

270 where β_0^* and β_1^* are calculated using generalized least squares regression. Figure 2 shows the
 271 difference in the trend lines resulting from SKLM and UK.

272 The semivariogram (i.e. variogram) is inversely related to the covariances between observations
 273 and provides the covariance matrix necessary for generalized least squares regression. A theoretical
 274 variogram function approximates the empirical variogram defined in this case as

$$275 \quad \hat{\gamma}(\mathbf{h}) = \frac{1}{2N_{h_1}} \sum_{\alpha_{h_1}=1}^{N_h} \left[r(\mathbf{u}_{\alpha_{h_1}}) - r(\mathbf{u}_{\alpha_{h_2}}) \right]^2 \quad (11)$$

276 where $\left[r(\mathbf{u}_{\alpha_{h_1}}), r(\mathbf{u}_{\alpha_{h_2}}) \right]$ represents each pair of regression model residuals located $\|\mathbf{h}\|$ distance
 277 away from each other. Figure 3 provides an example of the empirical and associated theoretical
 278 variograms for each dataset. It is the theoretical variogram that determines the values of the
 279 covariance function given in Equation 9.

280 Kriging predictions provide theoretical estimates of the prediction error uncertainty (often
 281 called kriging variance) (Moral 2010). A better understanding of prediction uncertainty could be
 282 used to make conservative adjustments to snow load predictions in volatile areas. Because error
 283 uncertainty cannot be compared across all methods, the authors leave the discussion of kriging
 284 variance as applied to snow load predictions to future work.

285 **CROSS VALIDATION**

286 This paper now proceeds with a comparison of the predictive accuracies of the previously
 287 described methods. Two common ways of measuring method accuracy are with new test data or
 288 cross validation. Test set error measures model accuracy on new observations not used in model
 289 fitting, which is often impractical as available observations beyond those used in model fitting are
 290 scarce. Cross validation seeks to approximate test set error without requiring additional data. This

291 is done by randomly dividing the given observations into groups, using all but one of these groups
292 to fit a model that makes predictions for the remaining group. This process is then repeated until
293 a prediction is made for each observation in the dataset. In this paper, the data are separated into
294 ten groups. Cross validation is a common tool used for model selection and refinement in many
295 disciplines (Arlot and Celisse 2010), including structural engineering (Chang et al. 2017) and will
296 be used to compare the spatial prediction methods defined in the preceding section.

297 The use of cross validation is limited to replicable methods that are separable from the input
298 observations. For example, snow load predictions in the Colorado snow load report involve a
299 contour map of input parameter values that includes allowed discontinuities along mountain ridges
300 (Torrents et al. 2016). These contours and discontinuities are inextricably connected to the station
301 observations and thus eliminate the option to use cross validation. In addition, the Montana and
302 Oregon snow load reports do not include enough details to replicate their methods on new datasets
303 (Theisen et al. 2004, NACSE 2012). Because of these limitations, the accuracy comparisons for
304 snow load prediction methods in these states are not included in the following results.

305 Cross validated errors are defined as

$$306 \quad E(\mathbf{u}_\alpha) = \hat{P}_g(\mathbf{u}_\alpha) - P_g(\mathbf{u}_\alpha) \quad (12)$$

307 where $\hat{P}_g(\mathbf{u}_\alpha)$ and $P_g(\mathbf{u}_\alpha)$ are the predicted and actual ground snow loads at station location
308 \mathbf{u}_α respectively. Defined in this way, a positive error indicates over-predictions and a negative
309 error indicates under-predictions. These errors are heteroskedastic and occasionally very large as
310 observed in Figure 4.

311 Overall comparisons of method accuracies are measured with mean absolute error (MAE) and
312 mean error (ME) defined similarly in Maguire et al. (2014) as

$$\begin{aligned} \text{MAE} &= \frac{1}{N} \sum_{\alpha=1}^N |E(\mathbf{u}_{\alpha})| \\ \text{ME} &= \frac{1}{N} \sum_{\alpha=1}^N E(\mathbf{u}_{\alpha}) \end{aligned} \tag{13}$$

where N represents the total number of weather stations with ground snow load measurements and $\hat{P}_g(\mathbf{u}_{\alpha})$ represents model predictions for each station location \mathbf{u}_{α} .

Parameter Selection

Many of the parameters associated with the previously described spatial prediction methods must be manually specified. In practice, values of these parameters are selected by cross validation. To illustrate such a procedure, Table 2 of Bean et al. (2017) selected PRISM parameters as follows:

- Create a vector of possible values for each of the eight PRISM parameters using recommendations from Daly et al. (2002).
- For every possible combination of the parameters, fit the PRISM model and record the prediction error (such as MAE) resulting from cross validation.
- Select a parameter combination that minimizes the prediction error.

Each dataset uses the log-PRISM parameters provided in Table 2 of Bean et al. (2017) during cross validation.

In addition, each dataset uses the Kriging variogram developed for UT-2017, rather than the dataset-specific variograms shown in Figure 3. Cross validation quantifies the effect of using a single variogram for predictions on ID-2015 and UT-1992. The MAE for ID-2015 and UT-1992 using the dataset-specific variograms in Figure 3 are within 0.01 kPa of the MAE using the UT-2017 variogram (as averaged over 100 iterations of cross validation). Such results show that the cross validated errors are fairly insensitive to modest changes in the theoretical variogram for SKLM and UK on the considered datasets.

334 **Error and Elevation**

335 The locally weighted regression (loess) (Cleveland and Devlin 1988) curves in Figure 5 reveal
336 the elevation dependent structure of the error scatter-plots previously shown in Figure 4. These
337 curves compute local weighted averages of raw and absolute station errors across elevation and
338 map these local averages as smooth polynomial curves. The gray tick marks drawn between each
339 set of plots represent the elevations of the individual stations locations. These tick marks help to
340 visualize station density across elevation. This characterization of density gives context to plotted
341 curves, as the loess estimates will be more reliable at elevations with a higher density of stations.

342 Figure 5 shows that PRISM, SKLM, and UK are fairly unbiased at low elevations (2000 meters
343 or less) and tend to under-predict at higher elevations (2000 - 3000 meters). The errors of all
344 methods are very unstable in ID-2015 at high elevations. The sinusoidal shape of the ME curves for
345 IDW reveal the tendency of this method to over-predict design ground snow loads at low elevations
346 and under-predict at high elevations. This behavior is a result of the relationship between NGSL
347 and elevation as discussed in the "Practical Limitations" section of this paper. Finally, Figure 5
348 shows the strong tendency of SNLW to over-predict design ground snow loads. In terms of relative
349 errors, the Utah equations on average predict design ground snow loads 34% higher than station
350 design ground snow load estimates from UT-2017 and 57% higher than estimates from UT-1992
351 (with median relative errors of 25% and 41% respectively). Recall that Equation 3 was intentionally
352 designed to over-predict design ground snow loads, and it is no surprise that this method would
353 have higher cross validated errors when compared to models designed to minimize error. However,
354 these accuracy comparisons are still useful as they quantify the magnitude of the over-prediction of
355 design ground snow loads using SNLW. Such over-predictions are understandable when considering
356 the consequences of under-predictions discussed earlier in this paper. However, reliability-based
357 engineering widely holds that snow load estimates should be as accurate and reliable as possible,
358 with conservative adjustments being made to load predictions through the selection of load factors
359 from a proper reliability analysis (Nowak and Collins 2012).

Accuracy Comparisons

Cross validated error measurements are partially subject to the random separation of observations into groups. To account for this randomness, cross validation is performed 100 times, recording the MAE and median absolute error (Med-AE) for each method at every iteration. The large difference between MAE and Med-AE illustrates the skewness invoked by the exceptionally high prediction errors that occasionally occur at high elevation locations. Figure 6 visualizes the average MAE and Med-AE of the 100 cross validation iterations. Black whiskers on each bar indicate the minimum and maximum MAE and Med-AE for the 100 iterations.

Figure 6 shows that PRISM, SKLM and UK notably outperform all other methods on both Utah datasets, with an MAE approximately 40-45% lower than SNLW and IDW on UT-2017. These improvements are not as pronounced for ID-2015, likely due to the less pronounced log-linear relationship between ground snow loads and elevation. However, the accuracy UK on ID-2017 remains notably better than all other methods, highlighting the accuracy improvements associated with the universal Kriging paradigm. These results demonstrate the accuracy improvements offered by PRISM and Kriging when compared to current snow load estimation methods used in Idaho and Utah. More importantly, the methodology used to obtain these results provides a pattern for comparing all snow load estimation methods used in the western states. Using cross validation in future snow load studies will provide state and federal officials with a universal and defensible standard for final model selections. Such a standard will ultimately improve the ground snow load estimation methods used across the region.

PRACTICAL LIMITATIONS

Figure 7 compares the current ground snow requirements in Utah to the predictions of PRISM, UK, and IDW. This comparison is an extension of a similar comparison provided in Bean et al. (2017). In many cases, the current predictions lead to a reduction in ground snow load requirements, with some major reductions occurring in places like Kamas, UT. In other cases, each of the methods recommended increased to the ground snow load requirements like Monticello, UT.

It is critical that these predictions and the previously discussed accuracy comparisons be placed

387 in the context of observational limitations. These predictions rely on accurate estimates of design
388 ground snow loads within each dataset and there is no guarantee that predictive accuracy for terrain
389 not represented in the input datasets will be comparable to cross validated accuracies reported
390 previously. The following subsections discuss some of the inevitable limitations associated with
391 predicting design ground snow loads.

392 **Limitations of Regression-Based Estimators**

393 There are extrapolation issues for the regression based estimators (PRISM, SKLM, UK, and
394 LR) when attempting to predict snow loads at locations with elevations far exceeding all nearby
395 station elevations. In Utah, these situations most often occur at mountain peaks lacking station
396 measurements. In such cases, these estimators begin to predict unreasonably high snow load values,
397 exceeding all observed snow load values in the dataset. This issue is resolved by restricting the
398 PRISM, Kriging, and IDW predictions to extend no higher than the largest design ground snow
399 load in the input dataset. In addition, the prediction of the global trend (as used in both kriging
400 estimators and linear regression) is not allowed to extend beyond the predicted trend for the highest
401 elevation station in the dataset. Such constraints are only imposed when predicting at the state level
402 and are not imposed for the cross validation results presented in this paper.

403 **Limitations of NGSL-Based Estimators**

404 Figure 7 reveals an alarming IDW prediction that is more than double the other method predic-
405 tions at Farmington, Utah (elevation 1316 meters). As observed in Table 2, three of the four stations
406 nearest to Farmington are all located at elevations above 2000 meters with NGSL several times
407 higher than the NGSL of the low elevation station. This results in a likely over-prediction of the
408 design ground snow load at Farmington and highlights a key shortcoming of using NGSL to account
409 for elevation. This shortcoming is due to the strong positive correlation between elevation and the
410 log transform of NGSL at station locations in Utah as observed in Figure 8. This correlation leads to
411 the sinusoidal error patterns for IDW observed previously in Figure 5. If NGSL fully accounted for
412 the effect of elevation on ground snow loads, then NGSL should be independent of elevation with a
413 non-significant correlation coefficient. However, the Pearson correlation coefficient associated with

414 Figure 8 is 0.63, which is highly statistically significant (p value < 0.0001). This correlation can be
415 insignificant globally yet significant locally. For example, the overall Pearson correlation between
416 elevation and log-NGSL on ID-2015 is only 0.14 (p value = .0004), while the Pearson correlation
417 for stations located in 12 counties comprising the south-eastern corner of the state, is 0.71 (p value
418 < .0001). The separation of locations into high and low elevation layers partially mitigates this
419 effect. For example, the 1219 m separating elevation used in the Idaho report (Al Hatailah et al.
420 2015) results in non-significant log-NGSL/Elevation correlations (i.e. p value > .01) of 0.05 and
421 0.35 for the low and high elevation layers in the ten counties comprising the Idaho panhandle.
422 However, this same separating elevation fails to eliminate the strong 0.71 correlation observed for
423 the 12 south-eastern counties, as all stations in this region are located in the upper elevation layer.

424 The prediction patterns associated with NGSL observed in Figures 5 and 7 are likely to occur
425 in topographically complex regions where the correlation between NGSL and elevation is strong.
426 Recalling the cost implications shown in Figure 1, differences in ground snow load prediction
427 similar in magnitude to those observed at Farmington, Utah could easily double or triple the cost
428 of the roof of a structure at these locations if this issue is not recognized and addressed.

429 **Limitations of 50 Year Estimates**

430 When fitting probability distributions to annual SWE maximums to predict 50 year ground
431 snow load events, the convergence rate of the estimated parameters via maximum likelihood is
432 on the order of $\mathcal{O}_p\left(n^{-\frac{1}{2}}\right)$ (Casella and Berger 2002). This means that a fourfold increase in the
433 sample size will reduce the estimation error by roughly half. However, the sample size necessary
434 to achieve an acceptable level of error will vary for every research project. The minimum number
435 of yearly observations required for distribution fitting were twelve in UT-2017, ten in ID-2015
436 (Al Hatailah et al. 2015), and seven in UT-1992 (SEAU 1992). These relatively small thresholds
437 for the distribution fitting process reflect practical efforts on the part of researchers to produce
438 reasonable 50 year estimates at stations with short periods of record. However, distributions fit
439 with only ten or so years of record are likely attempting to predict 50 ground snow loads with
440 magnitudes larger than all observations in the period of record.

441 Even with an "adequate" sample size, the inherently messy nature of real data (outliers, miss-
442 ing values, inaccurate measurements, and poor estimates of snow density from snow depth) adds
443 uncertainty to 50 year estimates. In addition, potential violations of two assumptions inherent to
444 the distribution fitting process add additional uncertainty to 50 year estimates. The first assumption
445 is that the yearly maximums at each station all come from the same distribution, implying that
446 the measurement conditions at each station location remain constant over the life of the station.
447 Documented changes in measurement tools, sampling site conditions, and human influence (Julan-
448 der and Bricco 2006) bring this assumption into doubt. The second assumption is that the yearly
449 maximums are statistically independent, implying that snow measurements at each station location
450 are uncorrelated across time. However, there is a wealth of evidence that suggests that time cannot
451 be ignored when measuring climatic events. Researchers claim that the proportion of precipitation
452 falling as snow in Utah has declined by nine percent in the last half century, accompanied by
453 long term decreases in overall snow cover (Gillies et al. 2012). This agrees with multiple sources
454 indicating that yearly snow packs are declining across the Pacific Northwest (Mote 2006, Scott
455 and Kaiser 2004). These sources indicate that the assumption of independence between yearly
456 maximums is most likely violated. These unaccounted sources of uncertainty are important to
457 acknowledge but difficult to quantify. The effect of such uncertainties will inevitably become more
458 prevalent when trying to predict recurrence intervals beyond 50 years, such as those explored in
459 Debock et al. (2017). Further work is required to determine precise influence these assumption
460 violations have on station ground snow load estimates.

461 One way to illustrate the effect of these uncertainties is through a comparison of estimated 50
462 year ground snow loads for COOP station USC00109638 in Weiser, Idaho (NOAA 2017). This
463 station was selected due to the series of snow related collapses occurring in Weiser during the
464 winter of 2017, where ground snow loads were estimated to be as high as 1.89 kpa (Arcement
465 2017). The reader should be cautioned that the reported collapses could be due to any number of
466 factors (design, construction, etc.), not just snow load prediction. The authors can not comment
467 on the safety of those structures, only to illustrate the uncertainty in 50 year ground snow load

468 based on the distribution and SWE prediction. Station records at this location extend as far back
469 as 1912. Data from this station were processed using the same procedures and filters used in the
470 creation of UT-2017, resulting in a sample size of 73 yearly maximum snow loads. The normal,
471 log-normal, gumbel and generalized extreme value (GEV) distributions each predict the 50 year
472 ground snow load estimate at this location, the latter two distributions being fit using the extRemes
473 package (Gilleland and Katz 2016). Efforts to fit a log-Pearson type III distribution via maximum
474 likelihood estimation were non-convergent and thus were excluded from the comparison. Each
475 distribution was fit twice: once using Sturm's equation to convert snow depths to SWE and again
476 using the RMCD. Table 3 compares each of the resulting 50 year estimates to the 0.81 kPa 50 year
477 ground snow load estimate in the Idaho snow load report.

478 Table 3 shows that different distributions can provide notably different estimates of 50 year
479 events. The differences in distribution estimates shown in Table 3 are relatively larger than
480 distribution comparisons at the Denver-Stapleton, Colorado snow site provided in DeBock et al.
481 (2017). Perhaps more important, however, is the difference in 50 year predictions resulting from
482 changes to the snow depth to SWE conversion method. Table 3 shows that, using the same
483 distribution, SWE estimates using Sturm's equation results are more than 50% higher than design
484 ground snow loads using RMCD. Differences of this magnitude are not unique to this particular
485 station, but are most pronounced at low elevation locations such as Weiser. Table 4 shows the
486 median absolute relative difference of 50 year estimates for 261 stations on UT-2017 relative to
487 the original log-normal distribution estimates. Of the 415 stations, 120 stations were excluded as
488 they did not require any SWE conversions and 21 stations were excluded for not having stable GEV
489 50 year estimates. These results confirm that differences in SWE conversion method are more
490 influential on design ground snow loads than differences in distribution selection. These large
491 differences reinforce the need for increased scrutiny in the process used to estimate design ground
492 snow loads.

493 **CONCLUSION**

494 Great care has been taken by each of the western states to develop ground snow load prediction

495 methods. However, little work has been done to formally compare the accuracy of these methods.
496 This paper began a formal comparison of methods using cross validation to compare a variety of
497 snow load prediction methods on three independently developed datasets for Utah and Idaho. The
498 cross validation results show that both Kriging methods and PRISM were the most accurate (in
499 terms of cross validated error) across all three datasets. For UT-2017, these methods had a 40-45%
500 lower mean absolute error the current method used in Utah and Idaho. Further, the cross validation
501 results show that UK performed the same as PRISM on the Utah datasets, but noticeably better than
502 PRISM on the ID-2015, suggesting that Universal Kriging may be the best method for predicting
503 ground snow loads across varying datasets. The relative ease of implementation for SKLM, UK,
504 and PRISM demonstrate the feasibility of using these methods on a consolidated dataset to make
505 predictions for multi-state regions. In addition, these prediction methods readily lend themselves
506 to other SWE-based topics, especially when making predictions across time. For example, the
507 authors have used PRISM to visualize changes in the water content of Utah's April 1st snow-pack
508 from 1930-2015.

509 This paper also discussed the limitations underlying the current distribution based methods for
510 estimating 50 year ground snow loads (or similar variants) at station locations. Comparisons of
511 various distributions and snow load conversion methods in Tables 3 and 4 show that estimated
512 design ground snow loads are very sensitive to changes in the SWE conversion method.

513 This in mind, the following conclusions can be made:

- 514 • SWE and distribution fitting assumptions provide differing design ground snow load station
515 predictions by up to a factor of nearly 290% based on the case study in Weiser, Idaho and
516 more than 40% on average when comparing stations from UT-2017.
- 517 • The top three considered methods (in terms of low cross validated MAE) account for log-
518 linear relationship between ground snow loads and elevation. The improvements in cross
519 validated accuracy using these methods was as much as 45% on UT-2017 when compared
520 to the current prediction methods used in Idaho and Utah.
- 521 • Normalized ground snow loads (NGSL) do not fully remove the effect of elevation in spatial

522 interpolation methods, with a Pearson correlation of 0.63 on UT-2017. This correlation,
523 when present, leads to a tendency for IDW to over-predict snow loads at low elevations, and
524 under-predict at high elevations.

- 525 • UK was similar in accuracy to PRISM on UT-2017 (MAE \approx 0.9kPa) and UT-1992 (MAE \approx
526 1.2kPa) and more accurate on ID-2015 (MAE \approx 1.4kPa vs MAE \approx 1.7kPa). Given its
527 relative simplicity, well defined prediction variance, and robustness to differences in input
528 data, the authors recommend Universal Kriging as the optimal method for predicting ground
529 snow loads in Utah and Idaho.

530 The framework for cross validation outlined in this paper can be readily adapted for larger scale
531 comparisons of snow load estimation methods across the country. Such a framework owes its
532 existence to the individual efforts of many of the western states, which have provided numerous
533 state-level ground snow load datasets for comparison. Leveraging these datasets for formal cross
534 comparisons of methods will accelerate the development of new and better models as well as the
535 improvement of existing ones. Consolidating the advancements made by each of the western states
536 will continue to improve the consistency and reliability in design ground snow load estimates across
537 the region.

538 **ACKNOWLEDGEMENTS**

539 The authors would like to thank the Structural Engineers Association of Utah, who provided
540 partial funding of the research conducted in this paper. The authors would also like to thank the
541 support of Bruce Brothersen and Jason Fisher at Vulcraft Utah for their help with contemporary
542 local costs.

543 **REFERENCES**

- 544 Akima, H. (1978). "A method of bivariate interpolation and smooth surface fitting for irregularly
545 distributed data points." *ACM Transactions on Mathematical Software (TOMS)*, 4(2), 148–159.
- 546 Akima, H. and Gebhardt, A. (2015). *akima: Interpolation of Irregularly and Regularly Spaced*
547 *Data*, <<https://CRAN.R-project.org/package=akima>>. R package version 0.5-12.

548 Al Hataillah, H., Godfrey, B. R., Nielsen, R. J., and Sack, R. L. (2015). “Ground snow loads for
549 Idaho–2015 edition.

550 Al Hataillah, H. A. (2015). “Ground Snow Loads for the State of Idaho.” M.S. thesis, University of
551 Idaho, Moscow, Idaho.

552 Arcement, K. (2017). “‘a lot of scared people’: Relentless snow collapses hundreds of Idaho roofs,
553 devastates rural county.” *The Washington Post*, <[https://www.washingtonpost.com/news/
554 morning-mix](https://www.washingtonpost.com/news/morning-mix/)> (January). Accessed: 05-15-2018.

555 Arlot, S. and Celisse, A. (2010). “A survey of cross-validation procedures for model selection.”
556 *Statistics surveys*, 4, 40–79 Accessed: 2017-09-08.

557 ASCE (2013). *Minimum Design Loads for Buildings and Other Structures*. American Society
558 of Civil Engineers, asce/sei 7-10 edition, <[http://ascelibrary.org/doi/abs/10.1061/
559 9780784412916](http://ascelibrary.org/doi/abs/10.1061/9780784412916)>.

560 ASCE (2017). *Minimum Design Loads and Associated Criteria for Buildings and Other Structures*.
561 American Society of Civil Engineers, asce/sei 7-16 edition, <[http://ascelibrary.org/
562 doi/abs/10.1061/9780784414248](http://ascelibrary.org/doi/abs/10.1061/9780784414248)>.

563 Associated Press (2017). “Roof on Provo building collapses under snow weight, <[https://www.
564 ksl.com/?nid=148&sid=42776523](https://www.ksl.com/?nid=148&sid=42776523)> (January). Accessed: 05-15-2018.

565 Bean, B., Maguire, M., and Sun, Y. (2017). “Predicting Utah ground snow loads with PRISM.”
566 *Journal of Structural Engineering*, 143(9), 04017126.

567 Bean, B., Maguire, M., and Sun, Y. (2018). “The Utah snow load study, <[https://
568 digitalcommons.usu.edu/cee_facpub/3589/](https://digitalcommons.usu.edu/cee_facpub/3589/)>. Accessed: 2017-09-08.

569 Casella, G. and Berger, R. L. (2002). *Statistical inference*, Vol. 2. Duxbury Pacific Grove, CA,
570 337,472.

571 Chang, M., Maguire, M., and Sun, Y. (2017). “Framework for mitigating human bias in selection
572 of explanatory variables for bridge deterioration modeling.” *Journal of Infrastructure Systems*,
573 23(3), 04017002.

574 Cleveland, W. S. and Devlin, S. J. (1988). “Locally weighted regression: an approach to regression

575 analysis by local fitting.” *Journal of the American statistical association*, 83(403), 596–610.

576 Daly, C., Gibson, W. P., Taylor, G. H., Johnson, G. L., and Pasteris, P. (2002). “A knowledge-based
577 approach to the statistical mapping of climate.” *Climate research*, 22(2), 99–113.

578 Daly, C., Halbleib, M., Smith, J. I., Gibson, W. P., Doggett, M. K., Taylor, G. H., Curtis, J.,
579 and Pasteris, P. P. (2008). “Physiographically sensitive mapping of climatological temperature
580 and precipitation across the conterminous United States.” *International Journal of Climatology*,
581 28(15), 2031–2064.

582 DeBock, D. J., Liel, A. B., Harris, J. R., Ellingwood, B. R., and Torrents, J. M. (2017). “Reliability-
583 based design snow loads. i: Site-specific probability models for ground snow loads.” *Journal of*
584 *Structural Engineering*, 04017046.

585 Ellis, S. (2017). “Snow damage to Idaho-Oregon onion industry nears
586 \$100 million, <[http://www.capitalpress.com/Idaho/20170127/
587 snow-damage-to-idaho-oregon-onion-industry-nears-100-million](http://www.capitalpress.com/Idaho/20170127/snow-damage-to-idaho-oregon-onion-industry-nears-100-million)> (January).
588 Accessed: 05-15-2018.

589 Fiscaro, K. (2017). “Snow-load removal began day before gym collapse.” *The*
590 *Observer*, <[http://www.lagrandeobserver.com/newsroomstafflist/5033603-151/
591 snow-load-removal-began-day-before-gym-collapse](http://www.lagrandeobserver.com/newsroomstafflist/5033603-151/snow-load-removal-began-day-before-gym-collapse)> (February). Accessed: 05-15-
592 2018.

593 Geis, J., Strobel, K., and Liel, A. (2011). “Snow-induced building failures.” *Journal of Performance*
594 *of Constructed Facilities*, 26(4), 377–388.

595 Gilleland, E. and Katz, R. W. (2016). “extRemes 2.0: An extreme value analysis package in R.”
596 *Journal of Statistical Software*, 72(8), 1–39.

597 Gillies, R. R., Wang, S.-Y., and Booth, M. R. (2012). “Observational and synoptic analyses of the
598 winter precipitation regime change over Utah.” *Journal of Climate*, 25(13), 4679–4698.

599 Glover, J. (2017). “Wet, heavy snow in Spokane sparks concern that weak
600 roofs could collapse, <[http://www.spokesman.com/stories/2017/feb/06/
601 wet-heavy-snow-in-spokane-sparks-concern-that-weak/#/0](http://www.spokesman.com/stories/2017/feb/06/wet-heavy-snow-in-spokane-sparks-concern-that-weak/#/0)> (February). Ac-

602 cessed: 05-15-2018.

603 Goovaerts, P. (1997). *Geostatistics for natural resources evaluation*. Oxford University Press.

604 Goovaerts, P. (2000). “Geostatistical approaches for incorporating elevation into the spatial inter-
605 polation of rainfall.” *Journal of hydrology*, 228(1), 113–129.

606 Julander, R. P. and Bricco, M. (2006). “An examination of external influences imbedded in the
607 historical snow data of Utah Accessed: 2018-05-15.

608 Kato, D. and Florio, G. (2017). “Montana theater’s roof collapses under weight of
609 snow, [http://billingsgazette.com/news/state-and-regional/montana/
610 montana-theater-s-roof-collapses-under-weight-of-snow/article_
611 5e61c0b7-c58d-5560-9b67-6a348da2d63f.html](http://billingsgazette.com/news/state-and-regional/montana/montana-theater-s-roof-collapses-under-weight-of-snow/article_5e61c0b7-c58d-5560-9b67-6a348da2d63f.html)> (February). Accessed: 05-15-2018.

612 Lafferty, K. (2017). “Snow buildup on porch roof causes collapse fa-
613 tally injuring Deary woman, [http://klewtelevision.com/news/local/
614 snow-buildup-on-porch-roof-causes-collapse-fatally-injuring-deary-woman](http://klewtelevision.com/news/local/snow-buildup-on-porch-roof-causes-collapse-fatally-injuring-deary-woman)>
615 (January). Accessed: 05-15-2018.

616 Maguire, M., Moen, C. D., Roberts-Wollmann, C., and Cousins, T. (2014). “Field verification of
617 simplified analysis procedures for segmental concrete bridges.” *Journal of Structural Engineer-
618 ing*, 141(1), D4014007.

619 Miere, E. (2017). “Snow causes partial roof collapse at Sears, Axis, Hole Bowl.” *Jack-
620 son Hole Daily*, [http://www.jhnewsandguide.com/jackson_hole_daily/local/
621 snow-causes-partial-roof-collapse-at-sears-axis-hole-bowl/article_
622 09e3f73d-cfcb-5be3-9462-a05f0fad1cce.html](http://www.jhnewsandguide.com/jackson_hole_daily/local/snow-causes-partial-roof-collapse-at-sears-axis-hole-bowl/article_09e3f73d-cfcb-5be3-9462-a05f0fad1cce.html)> (February). Accessed: 05-15-2018.

623 Moral, F. J. (2010). “Comparison of different geostatistical approaches to map climate variables:
624 application to precipitation.” *International Journal of Climatology*, 30(4), 620–631.

625 Moselle, B. (2016). *National Building Cost Manual 41st Edition*. Craftsman Book Company,
626 Carlsbad, CA (October).

627 Mote, P. W. (2006). “Climate-driven variability and trends in mountain snowpack in western North
628 America.” *Journal of Climate*, 19(23), 6209–6220.

629 NACSE (2012). “An updated snow load map and internet map server for Oregon (May).

630 Neuwirth, E. (2014). *RColorBrewer: ColorBrewer Palettes*, <[https://CRAN.R-](https://CRAN.R-project.org/package=RColorBrewer)

631 [project.org/package=RColorBrewer](https://CRAN.R-project.org/package=RColorBrewer)>. R package version 1.1-2.

632 NOAA (2017). “Cooperative observer network (COOP). Accessed: 2017-09-07.

633 Nowak, A. S. and Collins, K. R. (2012). *Reliability of structures*. CRC Press.

634 NRCS (2017). “Active SNOTEL stations, <www.wcc.nrcs.usda.gov/snow/sntllist.html>

635 (June).

636 Pebesma, E. J. (2004). “Multivariable geostatistics in S: the gstat package.” *Computers and Geo-*

637 *sciences*, 30, 683–691.

638 R Core Team (2017). *R: A Language and Environment for Statistical Computing*. R Foundation for

639 Statistical Computing, Vienna, Austria, <<https://www.R-project.org/>>.

640 Sack, R. L. (2015). “Ground snow loads for the western United States: State of the art.” *Journal of*

641 *Structural Engineering*, 142(1), 04015082.

642 Sack, R. L., Nielsen, R. J., and Godfrey, B. R. (2016). “Evolving studies of ground snow loads for

643 several western US states.” *Journal of Structural Engineering*, 04016187.

644 Sack, R. L. and Sheikh-Taheri, A. (1986). *Ground and roof snow loads for Idaho*. University of

645 Idaho, Department of Civil Engineering.

646 Scott, D. and Kaiser, D. (2004). “5.2 variability and trends in United States snowfall over the last

647 half century.

648 SEAU (1992). “Utah snow load study.

649 Strobel, K. and Liel, A. (2013). “Snow load damage to buildings: physical and economic impacts.”

650 *Proceedings of the Institution of Civil Engineers-Forensic Engineering*, 166(3), 116–133.

651 Sturm, M., Holmgren, J., and Liston, G. E. (1995). “A seasonal snow cover classification system

652 for local to global applications.” *Journal of Climate*, 8(5), 1261–1283.

653 Sturm, M., Taras, B., Liston, G. E., Derksen, C., Jonas, T., and Lea, J. (2010). “Estimating snow

654 water equivalent using snow depth data and climate classes.” *Journal of Hydrometeorology*,

655 11(6), 1380–1394.

656 Theisen, G. P., Keller, M. J., Stephens, J. E., Videon, F. F., and Schilke, J. P. (2004). “Snow loads
657 for structural design in Montana.

658 Torrents, J. M., DeBock, D. J., Harris, J. R., Liel, A. B., and Patillo, R. M. (2016). “Colorado
659 design snow loads.

660 USGS (2016). “Watershed boundary dataset, <<https://nhd.usgs.gov/wbd.html>>.

661 Utah Legislature (2016). *15A-3-107 Amendments to Chapter 16 of IBC*, <[https://le.utah.
662 gov/xcode/Title15A/Chapter3/15A-3-S107.html](https://le.utah.gov/xcode/Title15A/Chapter3/15A-3-S107.html)>. Accessed: 2018-05-15.

663 Wickham, H. (2009). *ggplot2: Elegant Graphics for Data Analysis*. Springer-Verlag New York,
664 <<http://ggplot2.org>>.

665
666
667
668
669
670
671
672
673
674
675
676
677
678
679
680
681
682
683

List of Figures

- 1 Cost to snow load comparison for five different roof joist types. 29
- 2 Station elevation plotted against design ground snow loads (log scale) for (a) UT-2017, (b) ID-2015, and (c) UT-1992. Lines for ordinary (OLS) and generalized least squares (GLS) are given in each case. In addition, (d) shows histograms of station elevations for each dataset. 30
- 3 Empirical (points) and theoretical (lines) semivariograms for each of the three datasets. 31
- 4 Scatter plot of cross validated errors for (a) PRISM, (b) SKLM, (c) SNLW, and (d) IDW on UT-2017. 32
- 5 Smoothed errors and absolute errors for (a) UT-2017, (b) UT-1992, and (c) ID-2015. The gray tick marks plotted along the x-axis of the three upper figures denote the individual station elevations. 33
- 6 Barchart of mean absolute errors (MAE) and median absolute errors (Med-AE) of spatial prediction methods for (a) UT-2017, (b) UT-1992, and (c) ID-2015. 34
- 7 Comparisons of spatial prediction methods to the 1992 Equations and recent 2016 amendments at select cities in Utah. 35
- 8 Station elevation plotted against NGSL (log scale), showing that there is still a clear (and unaccounted for) log-linear relationship between NGSL and elevation. 36

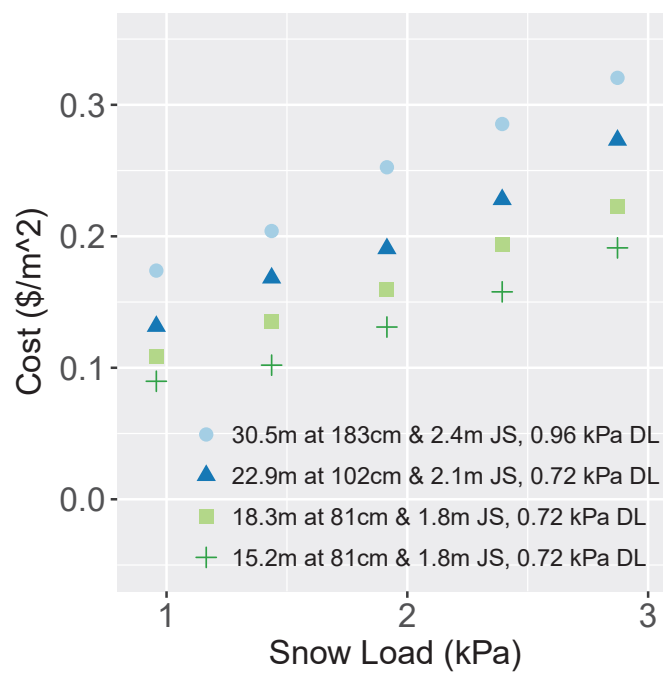


Fig. 1. Cost to snow load comparison for five different roof joist types.

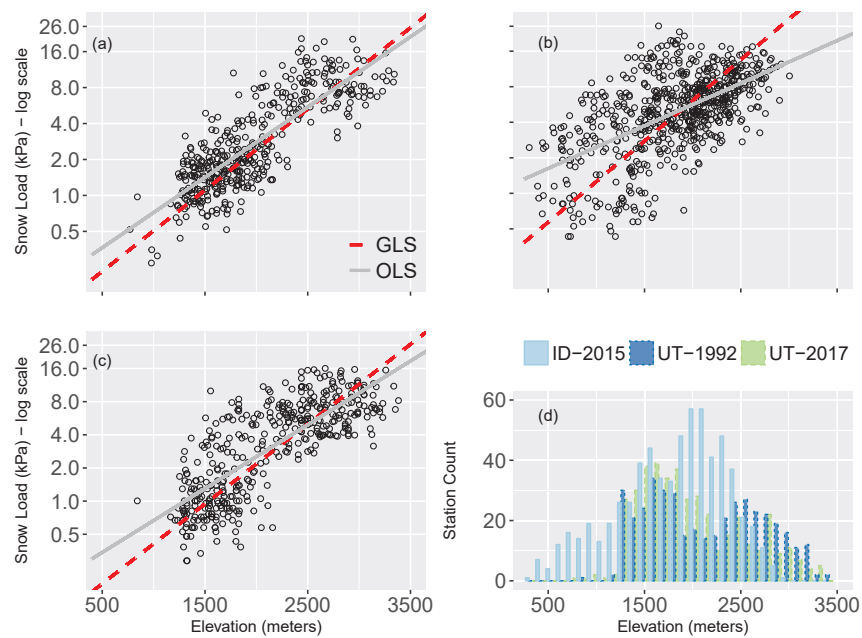


Fig. 2. Station elevation plotted against design ground snow loads (log scale) for (a) UT-2017, (b) ID-2015, and (c) UT-1992. Lines for ordinary (OLS) and generalized least squares (GLS) are given in each case. In addition, (d) shows histograms of station elevations for each dataset.

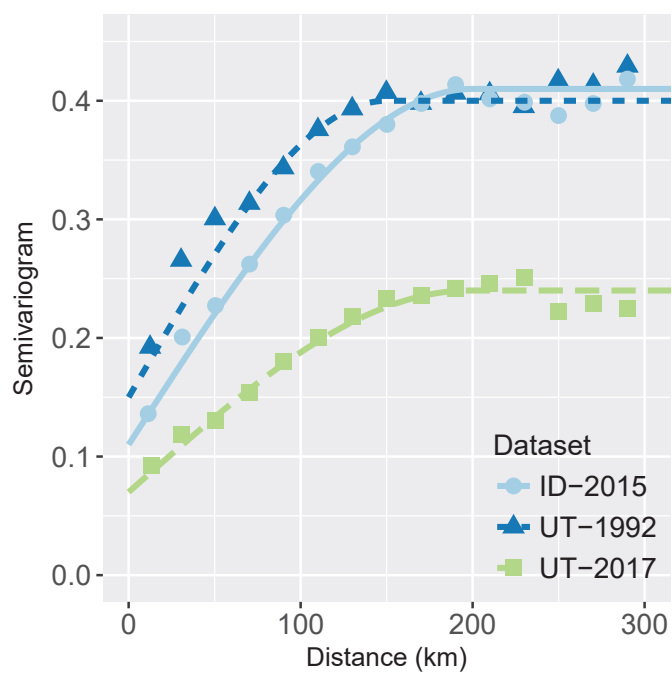


Fig. 3. Empirical (points) and theoretical (lines) semivariograms for each of the three datasets.

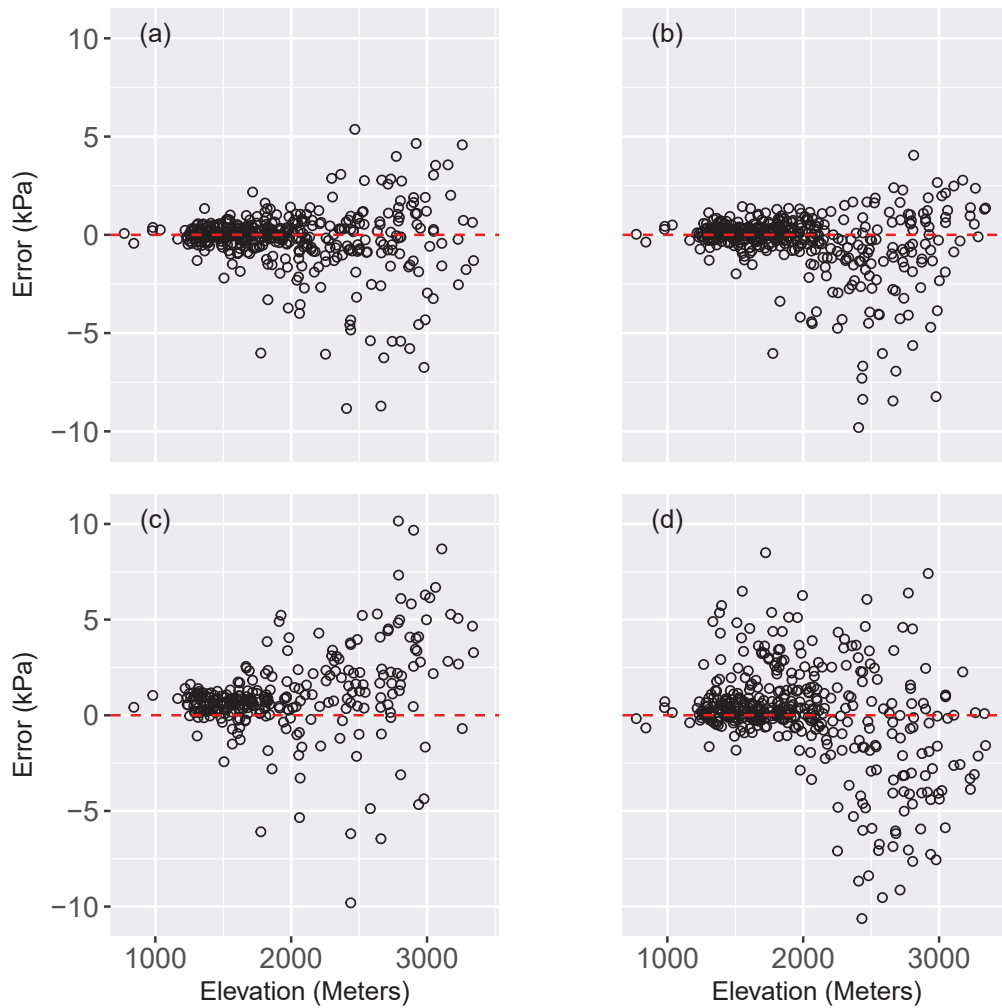


Fig. 4. Scatter plot of cross validated errors for (a) PRISM, (b) SKLM, (c) SNLW, and (d) IDW on UT-2017.

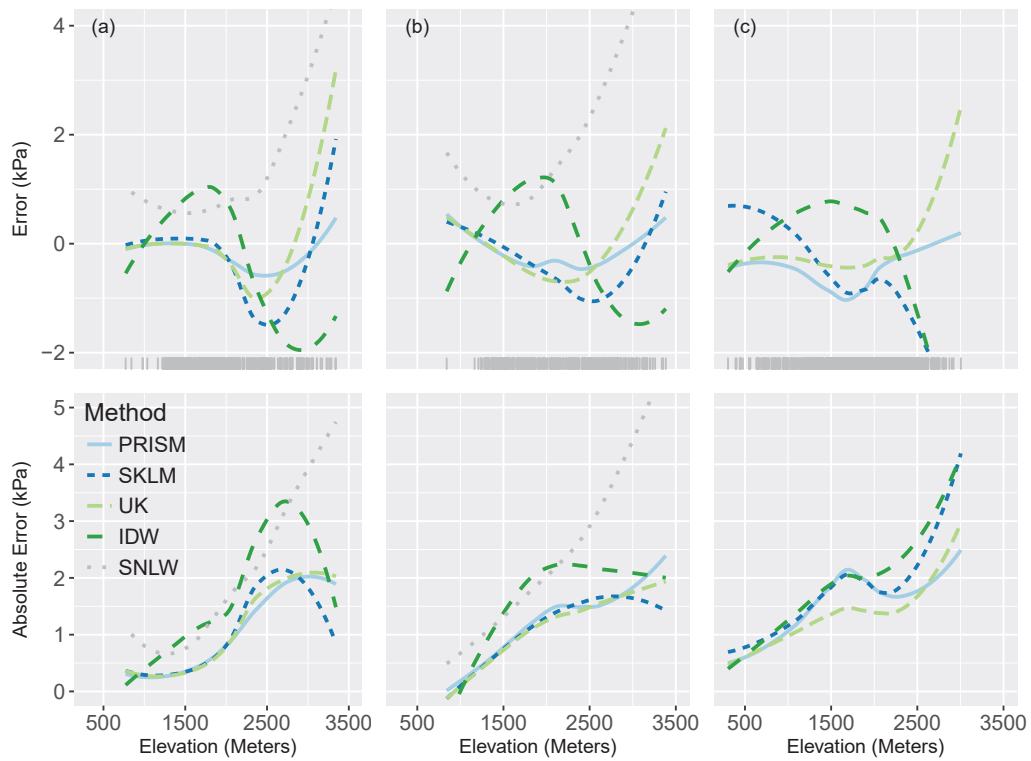


Fig. 5. Smoothed errors and absolute errors for (a) UT-2017, (b) UT-1992, and (c) ID-2015. The gray tick marks plotted along the x-axis of the three upper figures denote the individual station elevations.

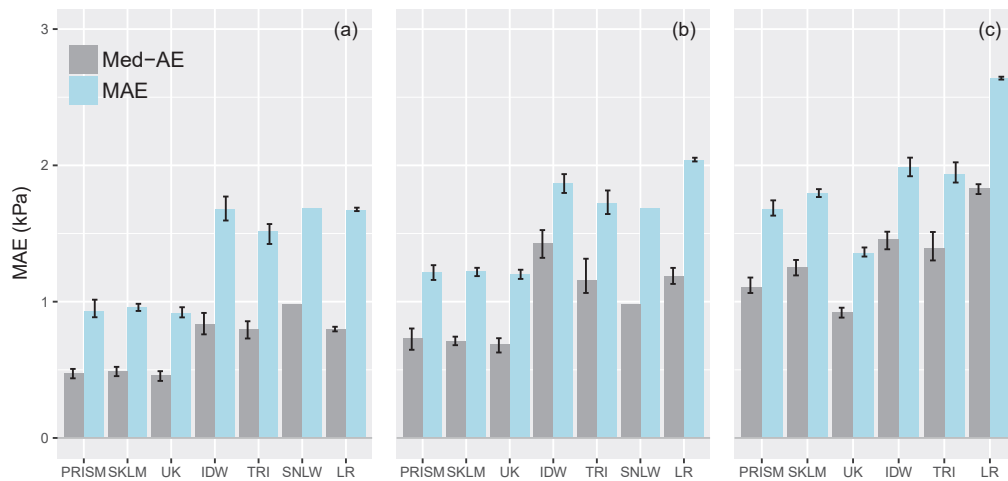


Fig. 6. Barchart of mean absolute errors (MAE) and median absolute errors (Med-AE) of spatial prediction methods for (a) UT-2017, (b) UT-1992, and (c) ID-2015.

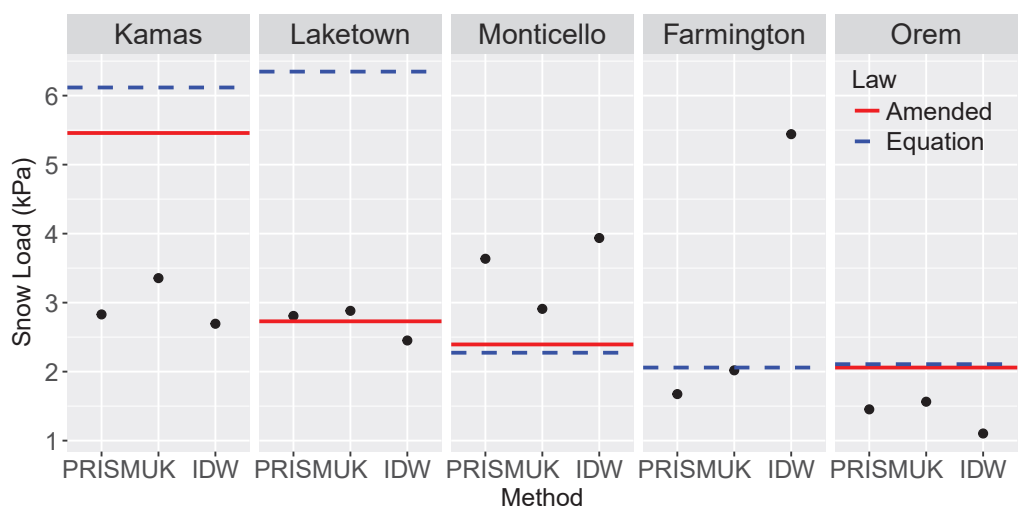


Fig. 7. Comparisons of spatial prediction methods to the 1992 Equations and recent 2016 amendments at select cities in Utah.

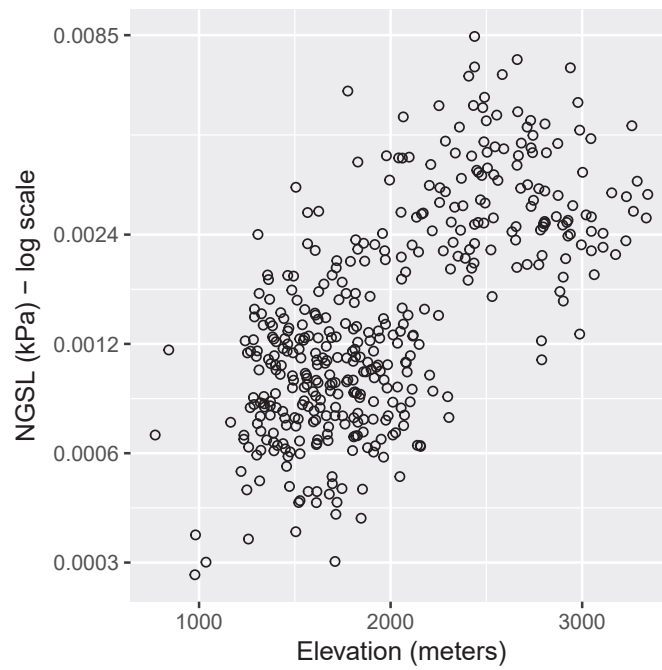


Fig. 8. Station elevation plotted against NGSL (log scale), showing that there is still a clear (and unaccounted for) log-linear relationship between NGSL and elevation.

684
685
686
687
688
689

List of Tables

1 Summary of the three design ground snow load datasets used in method comparisons. 38

2 NGSL at four nearest locations to Farmington, UT (111.884 W, 40.981 N). 39

3 50 year ground snow load estimates for Weiser, Idaho using a variety of distributions. 40

4 Median absolute relative difference in 50 year estimates as compared to original
log-normal distribution estimates. 41

TABLE 1. Summary of the three design ground snow load datasets used in method comparisons.

Dataset	Stations	SWE Conversions	Distribution
UT-2017	415	Sturn's Equation	Log-Normal
UT-1992	413	RMCD	Log-Pearson Type III
ID-2015	651	RMCD	Log-Pearson Type III

TABLE 2. NGSL at four nearest locations to Farmington, UT (111.884 W, 40.981 N).

Station	Elevation (m)	Distance to Location (km)	NGSL (kPa/m)
USC00422726	1335	5.4	0.0013
USS0011J11S	2438	5.5	0.0070
USS0011J12S	2066	6.4	0.0050
USS0011J68S	2359	8.4	0.0047

TABLE 3. 50 year ground snow load estimates for Weiser, Idaho using a variety of distributions.

Method	50 year estimate (kPa)	
	Sturm	RMCD
Log-Normal	1.64	1.04
Normal	1.54	1.07
Gumbel	1.55	0.99
GEV	2.34	1.25
Idaho Report		0.81

TABLE 4. Median absolute relative difference in 50 year estimates as compared to original log-normal distribution estimates.

Method	Absolute Relative difference (%)	
	Sturm	RMCD
log-Normal		35%
Normal	13%	42%
Gumbel	8%	40%
GEV	21%	29%